International Journal of the Physical Sciences Vol. 6(10), pp. 2497-2506, 18 May, 2011
Available online at http://www.academicjournals.org/IJPS
DOI: 10.5897/IJPS10.515
ISSN 1992 - 1950 ©2011 Academic Journals

Full Length Research Paper

Analysis of non-Newtonian blood flow through stenosed vessel in porous medium under the effect of magnetic field

Jagdish Singh and Rajbala Rathee*

Department of Mathematics, M.D. University, Rohtak (Haryana), India.

Accepted 21 April, 2011

The present study is analysis of non-Newtonian blood flow through stenosed vessel in porous medium. The blood is assumed to be pulsatile couple stress fluid. The effect of externally applied magnetic field on blood flow in porous medium is studied in the present analysis. The expressions of axial velocity, flow rate and shear stress have been obtained by using Laplace and finite Hankel transforms and their graphical interpretation has been discussed. The results obtained have been compared with previous studies in special cases and found to be in good agreement with other theoretical results.

Key words: Stenosed vessel, couple stress fluid, magnetic field, porous medium, finite Hankel transform, Laplace transform, axial velocity, shear stress.

INTRODUCTION

The study of blood flow in stenosed human arteries has been object of scientific research nowadays. Several researchers have considered blood as Newtonian fluid but some have also taken it as non-Newtonian. Since blood is a suspension of red blood cells in plasma, so it behaves as a non-Newtonian fluid at low shear rates. Lee and Fung (1970) analyzed Newtonian blood flow through stenosed artery. They have obtained numerical results of velocity, pressure, vorticity and shear stress in the range 0 to 25 of Reynolds number. Popel et al. (1974) supposed blood as a continuous media with couple stresses. They have taken into account the rotation and deformation of suspended particles. Mcdonald (1979) has discussed solution for approximate equations of steady flow through axially symmetric mild stenosed artery. Mehrotra et al. (1985) presented model of Newtonion blood flow in a stenosed artery of elliptical cross-section. They compared the results of velocity, pressure, shear stress and impedance with the results of tube of circular cross-section. Mishra and Chakravarty (1986) have studied the Newtonian flow of blood through arterial segment having a stenosis, considering the effect of surrounding orthotropic elastic connective tissue on the motion of wall.

Misra and Bar (1989) have developed mathematical model to study blood flow through stenosed blood vessel, by using momentum integral method taking into account the slip velocity at the wall of an artery and obtained analytical expressions for blood velocity, pressure gradient and skin fraction. Haldar and Ghosh (1994) have investigated Newtonian blood flow through indented artery under the effect of magnetic field in the presence of erythrocytes. They have taken variable blood viscosity according to Einstein relation and obtained expressions for blood velocity, pressure gradient, flow rate and have discussed graphically. Sanyal and Maji (1999) have discussed unsteady blood flow through stenosed artery with variable blood viscosity. Venkateswarlu and Rao (2004) have discussed numerical solution of unsteady blood flow through indented tube.

Dash et al. (1996) have analyzed Casson blood flow in homogeneous porous medium by employing Brinkman model. This analysis can model the real pathological condition of human artery. The main cause of formation of arterial stenosis is deposition of low density lipoprotein in arterial wall, since the surrounding tissue of blood vessel is porous and this intimal thickening of walls of artery leads to formation of stenosis. Chaturani and

*Corresponding author. E-mail: anjalisidharath@gmail.com.

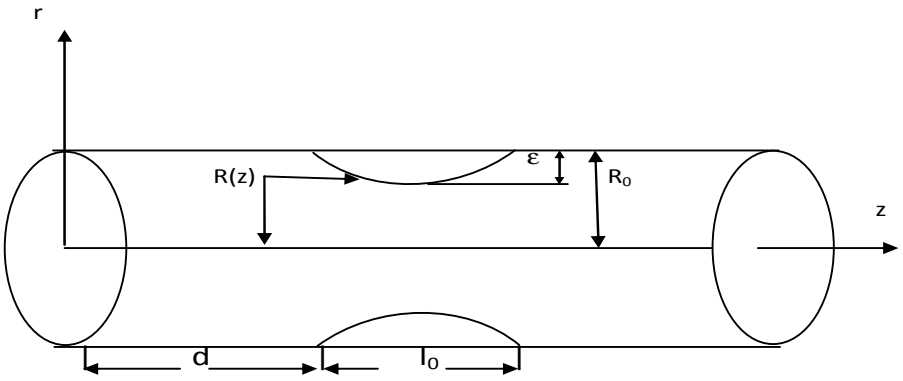

Figure 1. Geometry of the stenosed artery.

Upadhya (1977) have studied couple stress blood flow along inclined plane. Srivastava (1985) has studied couple stress blood flow through axially symmetric stenosed blood vessel and it is seen that shear stress is increased even in case of mild stenosis, when compared with the results of Newtonian fluid. Pralhad and Schultz (2004) studied couple stress fluid taken into account for both inertia and viscous terms. Singh and Rathee (2010) have analysed the two-dimensional blood flow through stenosed artery due to LDL effect in the presence of magnetic field. Singh et al. (2010) have discussed power law blood flow through radially non-symmetric multi-stenosed artery. Mishra and Verma (2010) discussed the effect of stenosis on non-Newtonian blood flow through uniform or non-uniform cross-section of blood vessels. They have considered blood as power law fluid, Bingham plastic fluid, Casson fluid and obtained analytic solution for different kinds of non-Newtonian fluids.

The effects of magnetic field and body acceleration on axial velocity of pulsatile blood flow in inclined circular tube have been discussed graphically by Sanyal et al. (2007). Rathod and Tanveer (2009) have discussed pulsatile flow of blood through a porous medium under the effect of magnetic field by considering blood as couple stress fluid through a straight and rigid circular tube using Laplace and Finite Hankel transform.

This model of blood flow is more realistic than other previous models because the medium sized arteries such as coronary arteries are more prone to atherosclerosis so, it would be more appropriate to consider blood fluid as non-Newtonian fluid. Here, we have analysed the effects of magnetic field on couple stress blood flow of constant viscosity μ and density ρ through stenosed blood vessel in porous medium. Since, recently the application of porous medium in blood flow through tissues has been considered as more appropriate because tissues are collection of dispersed cells. In the proposed model, we wish to examine the effect of porous medium and also the effect of magnetic field on couple stress blood flow.

MATHEMATICAL MODEL

In the present model, blood is represented by incompressible, homogeneous and pulsatile couple stress fluid in the presence of externally applied magnetic field through porous medium. We assume that induced magnetic field and electric fields are negligible. The flow is considered to be symmetric and fully developed. The geometry of stenosis is described by Haldar and Ghosh (1994) (Figure 1).

$$\frac{R(z)}{R_0} = 1 - A\left[l_0^{\,s-1}(z-d) - (z-d)^s \right], \quad d \le z \le d + l_0 \qquad (1)$$

where, s (≥2) is a parameter determining the shape of stenosis, d is the position of stenosis, l_0 is the length of stenosis, $R(z)$ is a radius of stenosed vessel, R_0 is radius of unobstructed blood vessel, z denote the axial positions and A is a parameter, given by

$$A = \frac{\varepsilon}{R_0\, l_0^{\,s}} \frac{s^{s/s-1}}{(s-1)}, \qquad (2)$$

ε is the maximum height of stenosis at $z = d + \dfrac{l_0}{s^{1/s-1}}$ such that $\varepsilon / R_0 << 1$.

The governing equation for the incompressible, pulsatile couple stress fluid under the effect of magnetic field in porous medium is given by

$$\mu \nabla^2 u - \eta_1 \nabla^2 (\nabla^2 u) - \sigma \beta_0^{\,2} u - \frac{\partial p}{\partial z} - \frac{\mu}{K} u = \frac{\partial u}{\partial T} \qquad (3)$$

$$\text{where } \nabla^2 \equiv \frac{1}{r}\frac{\partial}{\partial r}\left(r \frac{\partial}{\partial r} \right), \qquad (4)$$

$u(r,t)$ is velocity in the axial direction , β_0 is the external applied magnetic field, η_1 is a couple stress parameter. K is the

permeability of the isotropic porous medium and r is the radial coordinate. The boundary conditions, which support the present problem, are

$$\frac{\partial u}{\partial r} = 0 \text{ at } r = 0 \tag{5}$$

$$u = 0 \text{ at } r = R(z) \tag{6}$$

$$\frac{\partial^2 u}{\partial r} - \frac{\eta_1}{r}\frac{\partial u}{\partial r} = 0 \text{ at } r = R(z) \tag{7}$$

$$\frac{\partial^2 u}{\partial r} - \frac{\eta_1}{r}\frac{\partial u}{\partial r} \text{ is finite at } r = 0 \tag{8}$$

We use the transformation $y = r/R_0$ and $t = T\omega$ in Equation (3) in order to make the variables r and t dimensionless, so that

$$\frac{1}{y}\frac{\partial}{\partial y}\left(y\frac{\partial u}{\partial y}\right) - \frac{1}{\alpha_1^2}\frac{1}{y}\frac{\partial}{\partial y}\left[y\frac{\partial}{\partial y}\left\{\frac{1}{y}\frac{\partial}{\partial y}\left(y\frac{\partial u}{\partial y}\right)\right\}\right] - M^2 u - \frac{R_0^2}{\mu}\frac{\partial p}{\partial z} - \frac{R_0^2}{K}u = \alpha^2\frac{\partial u}{\partial t} \tag{9}$$

where,

$M^2 = \beta_0^2 R_0^2 \frac{\sigma}{\mu}$ is the Hartmann number ; $\alpha_1^2 = R_0^2 \frac{\mu}{\eta_1}$ is the Couple stress parameter; $\alpha^2 = R_0^2 \omega \frac{\rho}{\mu}$ is the Womersley parameter.

Integral transforms required for solution

If $f(y)$ satisfy Dirichlet conditions in closed interval $\left[0, R/R_0\right]$, then its finite Hankel transform is given by

$$u^*(\lambda_n) = \int_0^{R/R_0} y\,u(y)\,J_0(y\lambda_n)\,dy \tag{10}$$

where λ_n are the roots of $J_0\left(y\frac{R}{R_0}\right) = 0$. (11)

Its inverse Hankel transform is defined as

$$u(y) = 2\sum_{n=1}^{\infty} u^*(\lambda_n)\frac{J_0\left(y\lambda_n\right)}{J_1^2\left(\lambda_n\frac{R}{R_0}\right)}. \tag{12}$$

where, λ_n are positive roots of $J_0\left(\lambda_n\frac{R}{R_0}\right) = 0$, J_0 and J_1 are Bessel's functions of first kind. The Laplace transform of any function $f(t)$ is defined as:

$$\overline{f}(s) = \int_0^{\infty} e^{-st} f(t)\,dt, \qquad s > 0 \tag{13}$$

Analysis of the problem

The pressure gradient is defined as

$$-\frac{\partial p}{\partial z} = A_0 + A_1 \cos\omega T \tag{14}$$

Making use of transformation $t = T\omega$, Equation (14) becomes

$$-\frac{\partial p}{\partial z} = A_0 + A_1 \cos t \tag{15}$$

where A_0 is the steady part of the pressure gradient and A_1 is amplitude of the oscillatory part, $\omega = 2\pi f$ and f is the frequency of heart rate. Using Equation (15) in Equation (9), we get

$$\frac{1}{y}\frac{\partial}{\partial y}\left(y\frac{\partial u}{\partial y}\right) - \frac{1}{\alpha_1^2}\frac{1}{y}\frac{\partial}{\partial y}\left[y\frac{\partial}{\partial y}\left\{\frac{1}{y}\frac{\partial}{\partial y}\left(y\frac{\partial u}{\partial y}\right)\right\}\right] - M^2 u + \frac{R_0^2}{\mu}(A_0 + A_1 \cos t) - \frac{R_0^2}{K}u = \alpha^2\frac{\partial u}{\partial t} \tag{16}$$

Applying Laplace transform on Equation (16), we obtain

$$\alpha^2\left(s\overline{u}(y,s) - u(y,0)\right) = \frac{1}{y}\frac{\partial}{\partial y}\left(y\frac{\partial \overline{u}}{\partial y}\right) - \frac{1}{\alpha_1^2}\frac{1}{y}\frac{\partial}{\partial y}\left[y\frac{\partial}{\partial y}\left\{\frac{1}{y}\frac{\partial}{\partial y}\left(y\frac{\partial \overline{u}}{\partial y}\right)\right\}\right]$$

$$-M^2\overline{u} + \frac{R_0^2}{\mu}\left(\frac{A_0}{s} + \frac{A_1 s}{s^2+1}\right) - \frac{\mu}{K}\overline{u}(y,s) \tag{17}$$

Now, applying finite Hankel transform on Equation (17), we get

$$\overline{u}^*\left(\lambda_n, s\right) = \frac{\alpha_1^2 R R_0 J_1\left(\lambda_n\frac{R}{R_0}\right)}{\lambda_n \mu}\left[\frac{A_0 + A_1}{h_1(s+h_1/m)} + \frac{A_0}{m}\left\{\frac{m}{h_1 s} - \frac{m}{h_1(s+h_1/m)}\right\}\right.$$

$$\left. + \frac{A_1}{m}\left\{\frac{h_1 m s}{(h_1^2+m^2)(s^2+1)} + \frac{m^2}{(h_1^2+m^2)(s^2+1)}\right\} - \frac{A_1}{m}\frac{h_1 m}{(h_1^2+m^2)(s+h_1/m)}\right] \tag{18}$$

Also, taking inversion of both Laplace transform and finite Hankel transform, we obtain

$$u\left(y,t\right) = \frac{2\alpha_1^2 R R_0}{\mu}\sum_{n=1}^{\infty}\frac{J_0(\lambda_n y)}{\lambda_n J_1\left(\lambda_n\frac{R}{R_0}\right)}\left[\frac{A_0}{h_1} + A_1\left(\frac{1}{h_1} - \frac{h_1}{h_1^2+m^2}\right)e^{-\frac{h_1}{m}t}\right.$$

$$+\frac{A_1}{h_1^2+m^2}\left(h_1\cos t+m\sin t\right)\Bigg] \tag{19}$$

where,

$$h_1=\lambda_n^4+\alpha_1^2\left(\lambda_n^2+M^2+R_0^2/K\right) \tag{20}$$

$$m=\alpha^2\alpha_1^2. \tag{21}$$

The expression for flow rate Q is given by

$$Q=\frac{4\pi\alpha_1^2R^2R_0^2}{\mu}\sum_{n=1}^{\infty}\frac{1}{\lambda_n^2}\Bigg[\frac{A_0}{h_1}+A_1\left(\frac{1}{h_1}-\frac{h_1}{h_1^2+m^2}\right)e^{-\frac{h_1}{m}t}+\frac{A_1}{h_1^2+m^2}\left(h_1\cos t+m\sin t\right)\Bigg] \tag{22}$$

The shear stress at the wall is found to be

$$\tau_{rz}=-2\alpha_1^2RR_0\sum_{n=1}^{\infty}\Bigg[\frac{A_0}{h_1}+A_1\left(\frac{1}{h_1}-\frac{h_1}{h_1^2+m^2}\right)e^{-\frac{h_1}{m}t}+\frac{A_1}{h_1^2+m^2}\left(h_1\cos t+m\sin t\right)\Bigg] \tag{23}$$

Let us consider another case of pressure gradient, when

$$\frac{\partial p}{\partial z}=-A_0'e^{-\lambda t} \tag{24}$$

Then Equation (9) becomes,

$$\frac{1}{y}\frac{\partial}{\partial y}\left(y\frac{\partial u}{\partial y}\right)-\frac{1}{\alpha_1^2}\frac{1}{y}\frac{\partial}{\partial y}\left[y\frac{\partial}{\partial y}\left\{\frac{1}{y}\frac{\partial}{\partial y}\left(y\frac{\partial u}{\partial y}\right)\right\}\right]-M^2u+\frac{R_0^2}{\mu}A_0'e^{-\lambda t}-\frac{R_0^2}{K}u=\alpha^2\frac{\partial u}{\partial t} \tag{25}$$

Now, applying Laplace transform on Equation (25), we get

$$\frac{1}{y}\frac{\partial}{\partial y}\left(y\frac{\partial \bar{u}}{\partial y}\right)-\frac{1}{\alpha_1^2}\frac{1}{y}\frac{\partial}{\partial y}\left[y\frac{\partial}{\partial y}\left\{\frac{1}{y}\frac{\partial}{\partial y}\left(y\frac{\partial \bar{u}}{\partial y}\right)\right\}\right]-M^2\bar{u}+\frac{A_0'R_0^2}{\mu}\frac{1}{s+\lambda}-\frac{R_0^2}{K}\bar{u}=\alpha^2\left[s\bar{u}(y,s)-u(y,0)\right] \tag{26}$$

After employing finite Hankel transform, we find

$$\bar{u}^*(\lambda_n,s)=\frac{\alpha_1^2RR_0J_1\left(\lambda_n\frac{R}{R_0}\right)}{\lambda_n\mu}\Bigg[\frac{A_0'}{h_1(s+h_1/m)}+\frac{A_0'}{m}\Bigg\{\frac{1}{(h_1/m-\lambda)}\frac{1}{s+\lambda}-\frac{1}{(h_1/m-\lambda)(s+h_1/m)}\Bigg\}\Bigg].$$

Now, taking inversion of both Laplace transform and finite Hankel transform, we obtain

$$u(y,t)=\frac{2\alpha_1^2RR_0}{\mu}\sum_{n=1}^{\infty}\frac{A_0'J_0(\lambda_n y)}{\lambda_nJ_1\left(\lambda_n\frac{R}{R_0}\right)}\left[\left(\frac{1}{h_1}-\frac{1}{h_1-m\lambda}\right)e^{-\frac{h_1}{m}t}+\left(\frac{1}{h_1-m\lambda}\right)e^{-\lambda t}\right] \tag{27}$$

The flow rate Q is given by

$$Q=\frac{4\pi\alpha_1^2R^2R_0^2}{\mu}\sum_{n=1}^{\infty}\frac{A_0'}{\lambda_n^2}\left[\left(\frac{1}{h_1}-\frac{1}{h_1-m\lambda}\right)e^{-\frac{h_1}{m}t}+\left(\frac{1}{h_1-m\lambda}\right)e^{-\lambda t}\right] \tag{28}$$

The shear stress on the wall is obtained to be

$$\tau_{rz}=-2A_0'\alpha_1^2RR_0\sum_{n=1}^{\infty}\left[\left(\frac{1}{h_1}-\frac{1}{h_1-m\lambda}\right)e^{-\frac{h_1}{m}t}+\left(\frac{1}{h_1-m\lambda}\right)e^{-\lambda t}\right] \tag{29}$$

RESULTS AND DISCUSSION

The numerical experiment has been conducted by using MATLAB platform and the parameters which have been chosen for numerical computations are permeability constant 'K', magnetic field 'M', couple stress parameter 'α_1', and time 't'. The following parameter values have been used for graphical representations, that is, $A_0=2000$ dynes/cm^3, $A_1=4000$ dynes/cm^3, $L=100$ mm, $d=20$ mm, $l_0=40$ mm, $\mu=.035$ P, $\alpha=1$, $\alpha_1=2$. Figures 2 to 4 are drawn for axial velocity along the z-axis and it describes the variation of velocity at various times and Hartmann number. Figures 2 to 6 show variation of velocity profile (cm/time), flow rate (cm^3/time) and shear stress (dynes/cm^2) along z –axis (cm), when $-\frac{\partial p}{\partial z}=A_0+A_1Cost$. It is observed that, initially the velocity drops down and then increases slowly. Due to periodicity, there is fluctuation in the velocity for various times which is quite obvious in the real situations. For values of M = 1, 2, 3, 4 and 8, we see that as the time progresses, the effect of magnetic field is visualised to control the blood flow but beyond a certain magnitude of magnetic field, it is not advisable, as it may cause sudden death of patient as reported by Haldar and Ghosh (1994). Figure 3 is also for axial velocity along z-axis at α_1 =2, 4, 6, 8 and 10. In this case the trend of velocity with respect

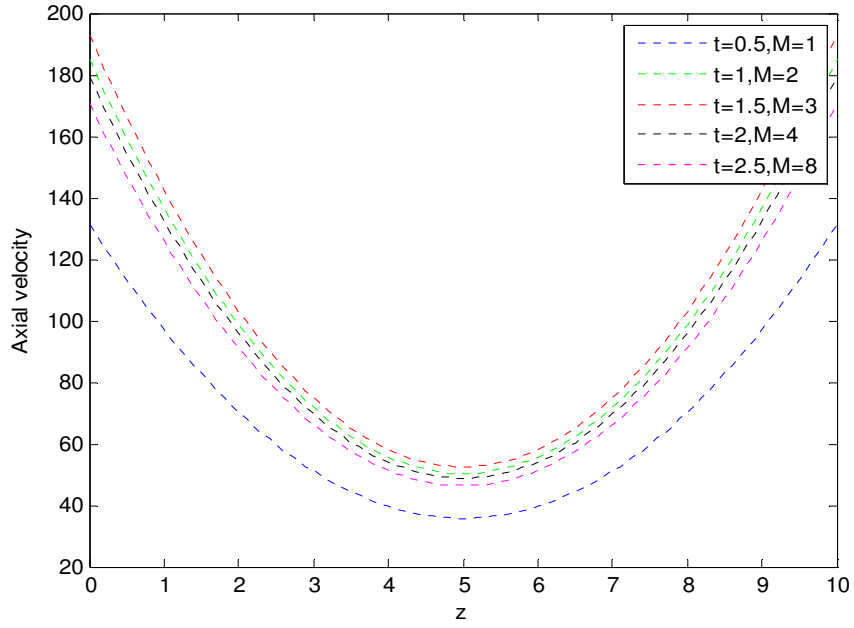

Figure 2. Variation of axial velocity at different values of time and Hartmann number.

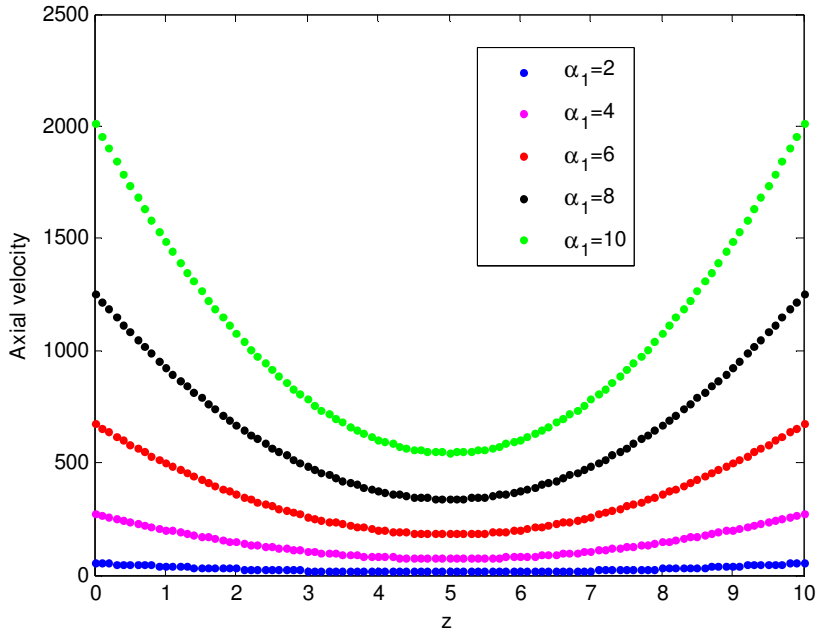

Figure 3. Variation of axial velocity along z-axis for different values of α_1.

to z-axis is same as in Figure 2, but it does not fluctuate. The effect of couple stress parameter is to increase the velocity which is desired in the vicinity of stenosis. Figure 4 shows the variation of velocity with increasing values of permeability 'K' and Hartmann number 'M'. The increase in velocity with increase in value of K depicts that the porosity increases the net uptake of LDL on the walls of arteries. This fact is also verified from Dash and Mehta (1996) that the velocity for the case of Casson fluid reflects the same behaviour for increase in values of K in tube without stenosis. Figures 5 represents the profiles for flow rate against 'z' wherein rate decreases sharply initially and then improves slowly. However, Figure 5 depicts that flow rate increases with increase in

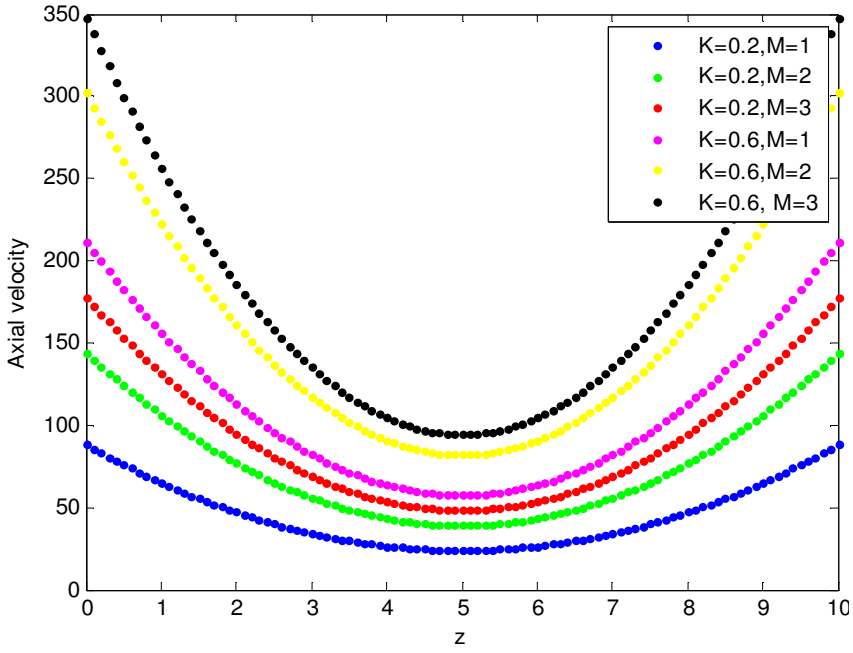

Figure 4. Variation of axial velocity along z-axis for different values of K and M .

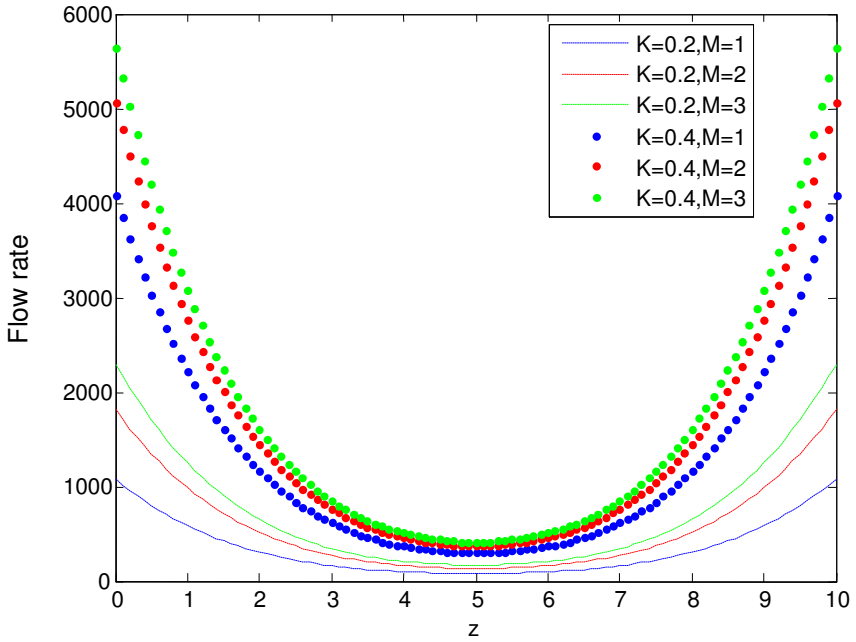

Figure 5. Variation of flow rate along z-axis for different values of K and M .

values of M and K respectively. Figures 6 to 8 are for variation of shear stress along z-axis. The shear stress increases sharply and then slows down moderately. It is maximum at the peak of stenosis. Figure 6 expresses the behaviour of shear stress for different values of time and M , but as the time increases, there is fluctuation for large values of M . Figure 7 describes the profiles of shear stress with different values of K and M . It increases with increase in values of both K and M . In Figure 8, the shear stress decreases with increase in

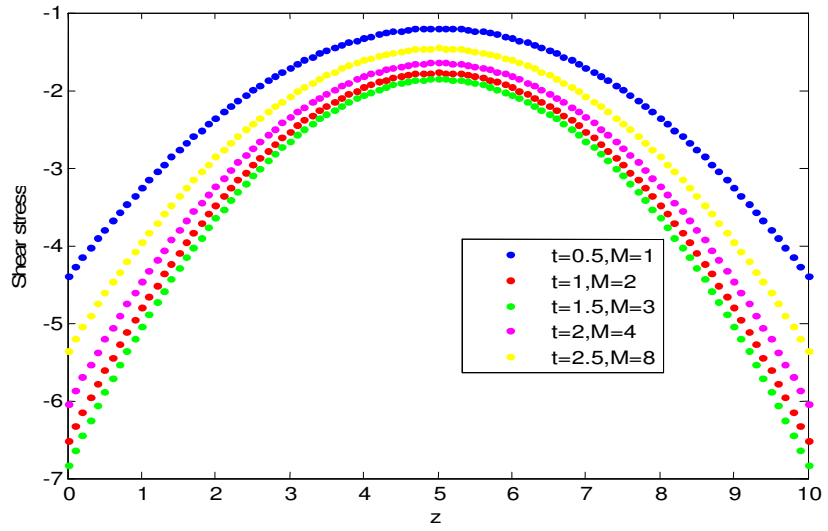

Figure 6. Variation of shear stress for different values of times and M.

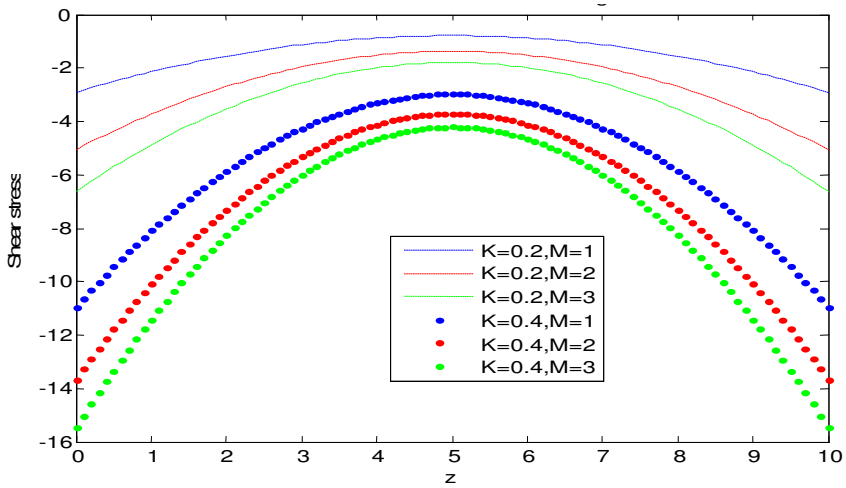

Figure 7. Variation of shear stress along z-axis for different values of K and M .

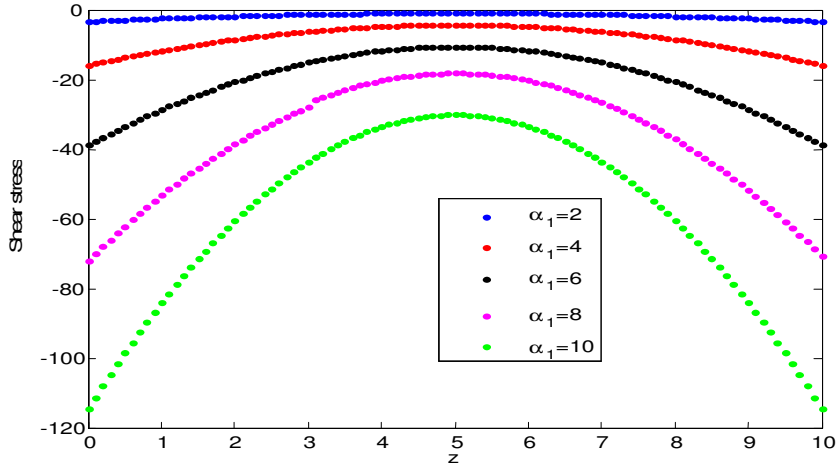

Figure 8. Variation of shear stress for different values of α_1 .

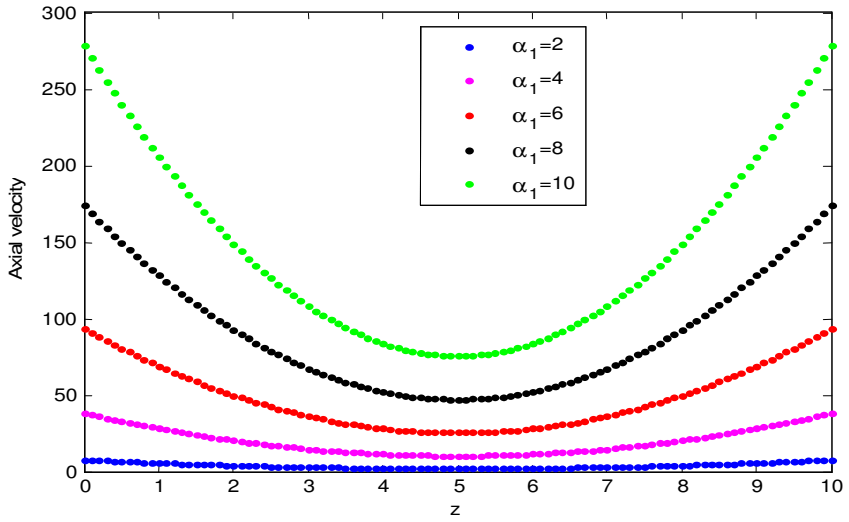

Figure 9. Variation of axial velocity along z-axis for different values of α_1.

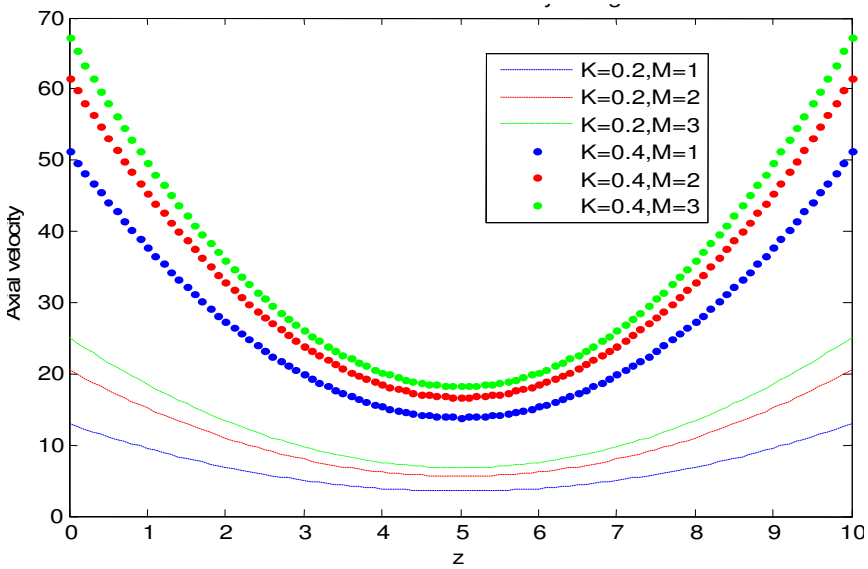

Figure 10. Variation of axial velocity along z-axis for different values of K and M.

values of couple stress parameter α_1 which is also reported by Srivastava (1985) and Pralhad and Schultz (2004). Figures 9 and 10 describe the trends of axial velocity for the pressure gradient $-\frac{\partial p}{\partial z} = A_0 ' e^{-\lambda t}$. The velocity first decreases sharply then increases moderately. However, the velocity increases with increase in values of α_1, K and M. Figures 11 and 12 show the profiles of shear stress along z-axis. Figure 9 to 12 show the variation of axial velocity (cm/time) and shear stress (dynes/cm^2), when $-\frac{\partial p}{\partial z} = A_0 ' e^{-\lambda t}$ The shear stress first increases and then decreases with respect to z. The stress decreases with increasing values of K, α_1, M, λ.

Conclusions

1. This analysis presents the results of axial velocity, flow rate, and shear stress graphically by considering the two

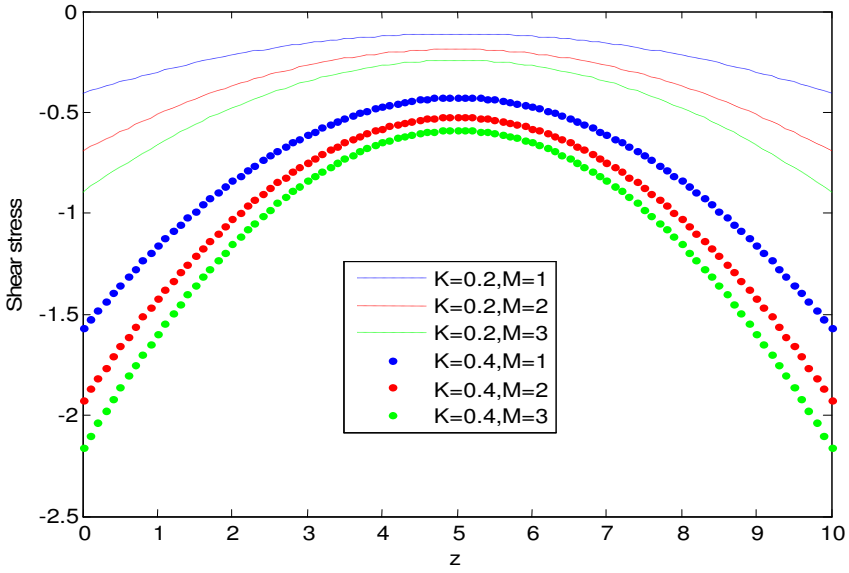

Figure 11. Variation of shear stress along z-axis for different values of K and M .

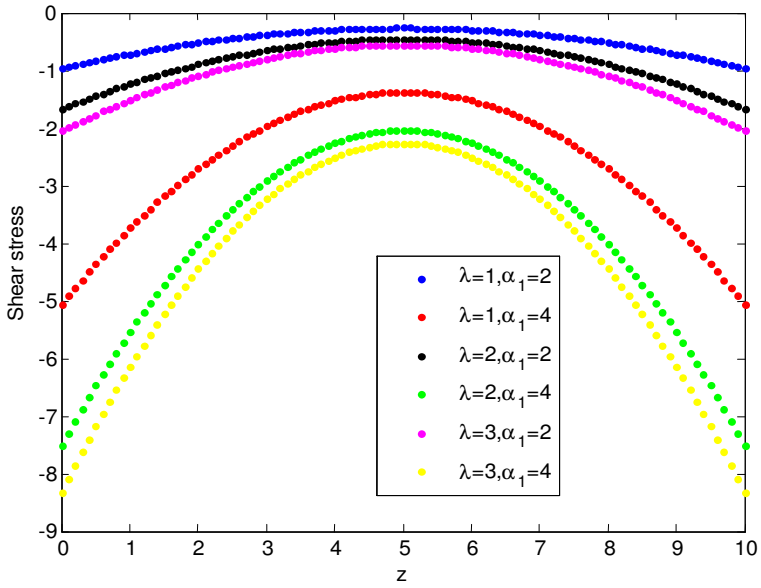

Figure 12. Variation of shear stress for different λ and α_1.

different pressure gradients. The same trends are observed for both forms of pressure gradient, but differ in magnitude.

2. The impact of porosity on blood flow leads to more and more deposition of LDL along the walls of arteries.

3. There are only fluctuations with increase in values of M and t .

4. The advantage of this study is that, we can calculate the extent of strength of magnetic field up to which we can control the blood flow in hypertensive patients and those who have blockage in their arteries.

5. This numerical experiment is helpful for biologists and medical practitioners to analyze the effects of magnetic field on the stenosed human arteries and to have precise information based on mathematical analysis and in the sense that, what magnitude of shear stress, a patient can bear having stenotic arteries, in case the magnetotherapy is used. Also, the blood pressure and velocity of the flow

can be precisely visualized on screen by making a suitable program based on this study.

REFERENCES

Lee JS, Fung YC (1970). Flow in locally constricted tubes at low Reynolds number. J. Appl. Mech., 37: 9-16.

Popel AS, Regirer SA, Usick PI (1974). A continuum model of blood flow. Biorheology, 11: 427-437.

Mcdonald DA (1979). On steady flow through modelled vascular stenoses. J. Biomech., 12: 13-20.

Mishra JC, Chakravarty S (1986). Flow in arteries in the presence of stenosis. J. Biomech., 19: 907-918.

Chaturani P, Upadhya VS (1978). Pulsatile of couple stress fluid through circular tubes with application to blood flow. Biorheology, 15: 193-201.

Mehrotra R, Jayaraman G, Padmanabhan N (1985). Pulsatile blood flow in a stenosed artery - A theoretical model. Med. Biol. Eng. Comput., 23: 55-62.

Srivastava LM (1985). Flow of couple stress fluid through stenotic blood vessels. J. Biomech., 18: 479-485.

Misra JC, Bar BK (1989). Momentum integral method for studying flow characteristic of blood through stenosed vessel. Biorheology, 26: 25-35.

Haldar K, Ghosh SN (1994). Effect of magnetic field on blood flow through indented tube in the presence of erythrocytes. Indian. J. Pure Appl. Math., 25(3): 345-352.

Dash RK, Mehta KN, Jayaraman G (1996). Casson fluid flow in a pipe filled with a homogeneous porous medium. Int. J. Eng., 34: 1145-1156.

Sanyal DC, Maji NK (1999). Unsteady blood flow through an indented tube with atherosclerosis. Indian J. Pure Appl. Math., 30(10): 951-959.

Pralhad RN, Schultz DH (2004). Modelling of arterial stenosis and its applications to blood diseases. Math. Biosci., 190: 203-220.

Venkateshwarlu K, Anand J (2004). Numerical solution of unsteady blood flow through an indented tube with atherosclerosis. Indian J. Biochem. Biophys., 41: 241-245.

Sanyal DC, Das K, Debnath S (2007). Effect of magnetic field on pulsatile blood flow through an inclined circular tube with periodic body acceleration. J. Phys. Sci., 11: 43-56.

Rathod VP, Tanveer S (2009). Pulsatile flow of couple stress fluid through a porous medium with periodic body acceleration and magnetic field. Bull. Malays. Math. Sci. Soc., 32(2): 245-259.

Singh B, Joshi P, Joshi BK (2010). Blood flow through an artery having radially non-symmetric mild stenosis. Appl. Math. Sci., 4: 1065-1072.

Mishra BK, Verma N (2010). Effect of stenosis on non-Newtonian flow of blood in blood vessels. J. Basic Appl. Sci., 4(4): 588-601.

Singh J, Rathee R (2010). Analytical solution of two-dimensional model of blood flow with variable viscosity through an indented artery due to LDL effect in the presence of magnetic field. Int. J. Phys. Sci., 5(12): 1857–1868.